Exploring the Design Space of Non-Planar Channels: Shape, Orientation, and Strain

Zlatan Stanojević*, Markus Karner†, and Hans Kosina*
*Institute for Microelectronics, TU Wien, Vienna, Austria; †Global TCAD Solutions GmbH, Vienna, Austria

Abstract

We conduct a comprehensive simulation study of non-planar n-type channels based on consistent, physical models containing measurable quantities rather than fit-parameters. This contrasts empirical thin-body models used in classical/quantum-corrected TCAD. The method involves the self-consistent solution of the two-dimensional Schrödinger-Poisson system, combined with linearized Boltzmann transport in the third dimension. We advance the art of simulation by (i) introducing quantum simulation on unstructured meshes for arbitrary geometries, (ii) providing an efficient framework for rapid evaluation of device designs, and (iii) contributing a surface roughness scattering model for arbitrarily shaped surfaces. Consistent modeling allows us to make reliable assertions with respect to device performance.

Introduction

As MOSFET channels have gone 3D, new degrees of freedom in design and fabrication have appeared, raising several questions: What is the best combination of channel/substrate orientation? How does surface roughness affect carrier transport? What strain conditions will enhance channel mobility? Is there any performance to be gained from tapered tri-gate channels?

State of the Art – Empirical Modeling

The questions are typically addressed using classical TCAD simulation with empirical models for planar technologies which brings up the following problems: (i) Quantum correction models like density gradient need to be calibrated for each doping and oxide thickness and fail for very thin channels. (ii) Mobility models like the Lombardi model (1) and even more advanced ones including 2DEG scattering in inversion/accumulation (IALMob) (2), (3) are calibrated using planar MOS or UTB data of one particular surface orientation, requiring one set of parameters for each orientation. (iii) Strain is incorporated in post processing by empirical piezoresistivity models, practically demanding re-calibration for every device and stress configuration.

Physical Modeling

In this work, we address the aforementioned questions on a physical level. To this end, we have developed a novel set of modeling and simulation tools that yields a *consistent* picture for all device variations, allowing direct and *consistent* comparison of designs. Our approach relies on a minimal set of material properties, that are either well known or measurable, instead of fit-parameters, while still being as efficient as state-of-the-art TCAD device simulation. The implementation is realized within the Vienna Schrödinger-Poisson (VSP) simulator (4), part of GTS Framework (5).

A. Schrödinger-Poisson

We assume two-dimensional quantum confinement inside the non-planar channel and model the electronic structure in the cross section solving the 2D Schrödinger equation in the effective mass approximation (EMA) as well as with a $\mathbf{k}\cdot\mathbf{p}$ band structure (4). The use of unstructured grids and anisotropic discretization naturally captures the effects of channel shape and orientation (6). For the electronic band structure, a two-band $\mathbf{k}\cdot\mathbf{p}$ Hamiltonian is used (7) that has been validated using ab-initio calculations (8). The effect of strain is included via deformation potentials for EMA and $\mathbf{k}\cdot\mathbf{p}$.

B. Carrier Scattering

The low-field conductivity/mobility of the channels is computed from the linearized Boltzmann transport equation (L-BTE) and serves as a *metric* to rate and compare device performance. It represents the diffusive limit or *worst case* for transport, i.e. a real, short-channel device will have a higher current. Phonon and surface roughness scattering (SRS) are considered the dominant scattering mechanisms at 300 K. A novel SRS model (9) is used; it extends the model of Prange and Nee (10) with respect to non-planar geometries and band anisotropy. Axial and lateral momentum transfer are accurately taken into account. Central to the SRS model are matrix elements that vary across the surface, called *form functions* $f_{n,n';k,k'}(s)$ with s being the surface coordinate. The transition rate is calculated using

$$S_{n,n'}(k,k') = \frac{1}{\hbar L}\int_{\mathbb{R}} |F_{n,n';k,k'}(q_\perp)|^2 C(q)\mathrm{d}q_\perp \; \delta(E_{n'}(k') - E_n(k)), \quad (1)$$

where $F_{n,n';k,k'}(q_\perp)$ are the Fourier transformed form functions and $C(q)$ is the roughness power spectrum ($q = \sqrt{(k-k')^2 + q_\perp^2}$). The procedure is outlined in Fig. 2.

Results

We start by investigating the transfer characteristic of Intel's tri-gate device (11) (Fig. 3) for different combinations of channel and substrate orientation. We find that channel conductivity severely degrades (Fig. 4) for the orientations $[110]/(001)$ and $[110]/(1\bar{1}1)$ but not for $[110]/(1\bar{1}0)$ and $[100]/(010)$, the latter being the traditional channel orientation for Si MOSFET devices. To find the reason and whether

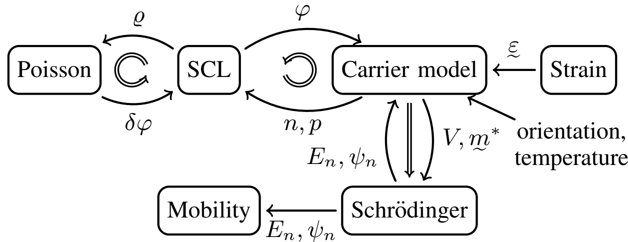

Fig. 1. The flexible architecture of the VSP allows to arrange complex simulation flows. Shown are the models involved in the computations performed in this work: a self-consistent Schrödinger-Poisson loop (SCL) is run with strain and mobility models as pre and post-processing steps, respectively. Single arrows represent data flow, double arrows control flow.

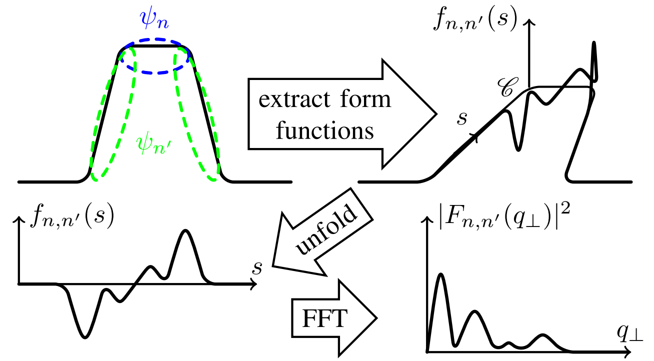

Fig. 2. Computational procedure to obtain the surface roughness scattering rates. For each two cross-section wavefunctions ψ_n and $\psi_{n'}$ the position-dependent matrix element (form function $f_{n,n'}(s)$) is evaluated along the interface curve $\mathscr{C}$ on the mesh. The sqare magnitude of their Fourier transform, $F_{n,n'}(q_\perp)$, is multiplied by the roughness power spectrum and integrated to give the scattering rate.

tapering has any influence, we conduct a systematic study on an ensemble of different channel shapes, ranging from triangular via trapezoidal to rectangular (Fig. 5). A differential analysis of the contributing scattering mechanisms in Fig. 6 reveals that SRS is the source of mobility degradation: In the rectangular channel electrons interact with both top and sidewall roughness; in the triangular channel they are squeezed between the inclined sidewalls. Proximity to rough $\{110\}$ or $\{111\}$ surfaces is known to reduce electron mobility, compared to $\{100\}$ (12). Hence, if the interacting surfaces are not close to $\{100\}$, mobility degradation will occur.

While $[110]/(1\bar{1}0)$ appears merely as good as $[100]/(010)$ in the EMA approximation, $\mathbf{k}\cdot\mathbf{p}$-analysis of the subband structure (Fig. 8) reveals that $[100]/(010)$ has reduced mobility due to increased transport effective mass; the mass increase is due to confinement and cannot be mitigated by strain. $[110]/(1\bar{1}0)$ on the other hand not only shows little to no transport mass increase but its mass can be reduced below bulk level using tensile stress along the channel (Fig. 9), resulting in an mobility enhancement of $\approx 30\%$ for $600\,\mathrm{MPa}$ which is in excellent agreement with experimental data (13).

Conclusion

We present a comprehensive modeling approach for investigating the design space of non-planar MOSFET channels, spanned by channel shape, crystal orientation, and strain, based on physical modeling.

We observe a complex interplay between orientation and surface roughness that in many cases leads to severe degradation of device performance. Our study shows $[110]/(1\bar{1}0)$ as only alternative orientation to $\langle 100\rangle$ that does not suffer from mobility degradation through SRS and moreover allows additional mobility enhancement of 30% and possibly more.

Acknowledgment

This work has been supported by the Austrian Science fund through contracts F025 and I841-N16.

References

(1) C. Lombardi, S. Manzini, A. Saporito, and M. Vanzi. "A physically based mobility model for numerical simulation of nonplanar devices." *IEEE T. Comput. Aid. D.*, vol. 7(11), pp. 1164–1171, 1988.
(2) S. Reggiani, E. Gnani, A. Gnudi, M. Rudan, and G. Baccarani. "Low-Field Electron Mobility Model for Ultrathin-Body SOI and Double-Gate MOSFETs With Extremely Small Silicon Thicknesses." *IEEE T. Electron. Dev.*, vol. 54(9), pp. 2204–2212, 2007.
(3) "Synopsys TCAD News Apr.", April 2013.
(4) Z. Stanojevic and H. Kosina. "VSP - a Quantum Simulator for Engineering Applications." In *Intl. Workshop Comput. Electron.*. June 2013, pp. 93–94.
(5) http://www.globaltcad.com/en/products/gts-framework.html
(6) Z. Stanojevic, M. Karner, K. Schnass, C. Kernstock, O. Baumgartner, and H. Kosina. "A versatile finite volume simulator for the analysis of electronic properties of nanostructures." In *Proc. 16th SISPAD*. Sept 2011, pp. 143–146.
(7) J. C. Hensel, H. Hasegawa, and M. Nakayama. "Cyclotron Resonance in Uniaxially Stressed Silicon. II. Nature of the Covalent Bond." *Phys. Rev.*, vol. 138(1A), pp. A225–A238, Apr 1965.
(8) V. A. Sverdlov, T. Windbacher, F. Schanovsky, and S. Selberherr. "Mobility Modeling in Advanced MOSFETs with Ultra-Thin Silicon Body under Stress." *JICS*, vol. 4(2), pp. 55–60, 2009.
(9) Z. Stanojevic and H. Kosina. "Surface-Roughness-Scattering in Non-Planar Channels – the Role of Band Anisotropy." In *Proc. 18th SISPAD*. Sept 2013, pp. 352–355.
(10) R. E. Prange and T.-W. Nee. "Quantum Spectroscopy of the Low-Field Oscillations in the Surface Impedance." *Phys. Rev.*, vol. 168, pp. 779–786, Apr 1968.
(11) C. Auth, C. Allen, A. Blattner, D. Bergstrom, M. Brazier, M. Bost, et al. "A 22nm high performance and low-power CMOS technology featuring fully-depleted tri-gate transistors, self-aligned contacts and high density MIM capacitors." In *VLSIT*. 2012, pp. 131–132.
(12) S. Takagi, A. Toriumi, M. Iwase, and H. Tango. "On the universality of inversion layer mobility in Si MOSFET's: Part II-effects of surface orientation." *IEEE T. Electron. Dev.*, vol. 41(12), pp. 2363–2368, 1994.
(13) S. Bangsaruntip, A. Majumdar, G. Cohen, S. Engelmann, Y. Zhang, M. Guillorn, et al. "Gate-all-around silicon nanowire 25-stage CMOS ring oscillators with diameter down to 3 nm." In *VLSIT*. 2010, pp. 21 –22.
(14) Chipworks Tech. Blog. "Intel's 22-nm Tri-gate Transistors Exposed.", April 2012.
(15) Z. Stanojevic, V. Sverdlov, O. Baumgartner, and H. Kosina. "Subband engineering in n-type silicon nanowires using strain and confinement." *SSE*, vol. 70(0), pp. 73 – 80, 2012.

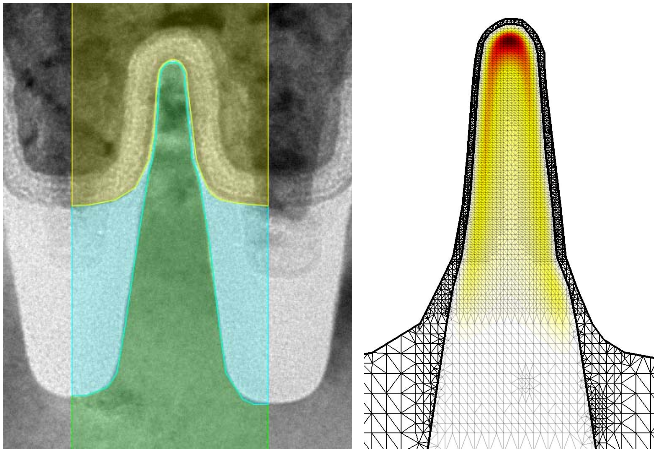

Fig. 3. Left: TEM image of an NMOS fin structure fabricated by Intel (11), (14); segments of the simulation domain are overlaid. Right: electron concentration in the fin under gate bias $V_{\mathrm{G}} = 1\,\mathrm{V}$ from a self-consistent Schrödinger-Poisson calculation; the computational grid is shown.

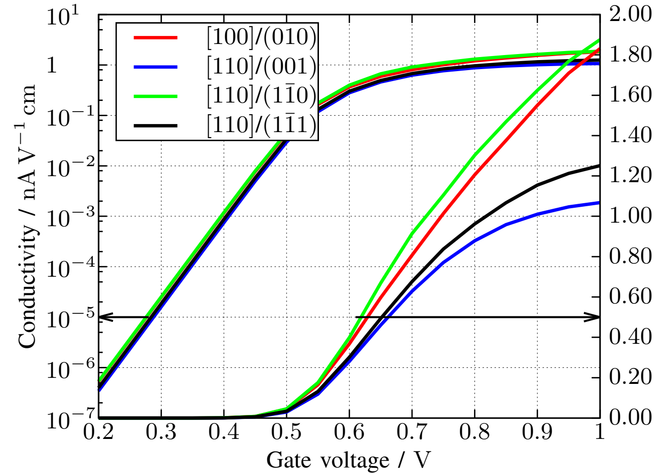

Fig. 4. Fin channel transfer characteristics for four different channel/substrate orientations of the device shown in Fig. 3; degradation of the characteristic can be observed for [110]/(001) and [110]/(1$\bar{1}$1) orientations, but not for [110]/(1$\bar{1}$0) which has about the same drive current as [100](010), the traditional orientation in Si MOSFET fabrication.

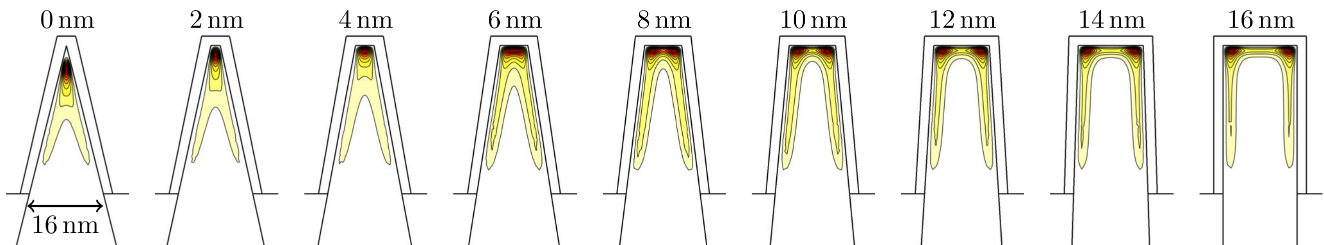

Fig. 5. To shed light on what influences current degradation, an ensemble of channel cross-section shapes is generated, ranging from a triangular fin to rectangular one. Transfer characteristics are calculated for each shape and orientation; electron concentration is shown for the [110]/(001) orientation (degraded) at $V_{\mathrm{G}} = 1\,\mathrm{V}$ (strong inversion). We note that electrons preferably occupy the top of the fin and the device corners with slight inversion close to the sidewalls.

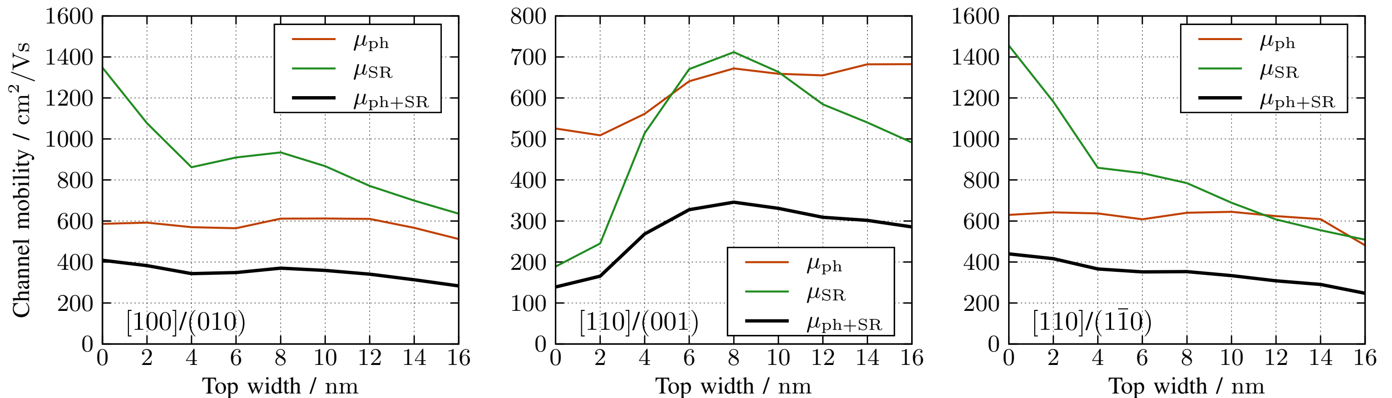

Fig. 6. Breaking down the mobility into the contributing scattering mechanisms reveals that surface roughness scattering (SRS) is mainly responsible for the orientation-dependent behavior. SRS-limited mobility increases with thinning of the fin top for [100]/(010). In [110]/(001) direction the picture is quite different: SRS-limited mobility increases with tapering, reaching a local maximum and then plummeting as the triangular shape is approached; [110]/(1$\bar{1}$0) does not appear to suffer from increased SRS and exhibits almost the same behavior as [100]/(010). The explanation for this is that electrons scatter more off rough {110} and {111} surfaces than they do off {100} surfaces (12). In the [100]/(010) and [110]/(1$\bar{1}$0) channels electrons face the rough sidewalls roughly at {100}, while in the [100]/(001) channel sidewall are approximately {110}-oriented.

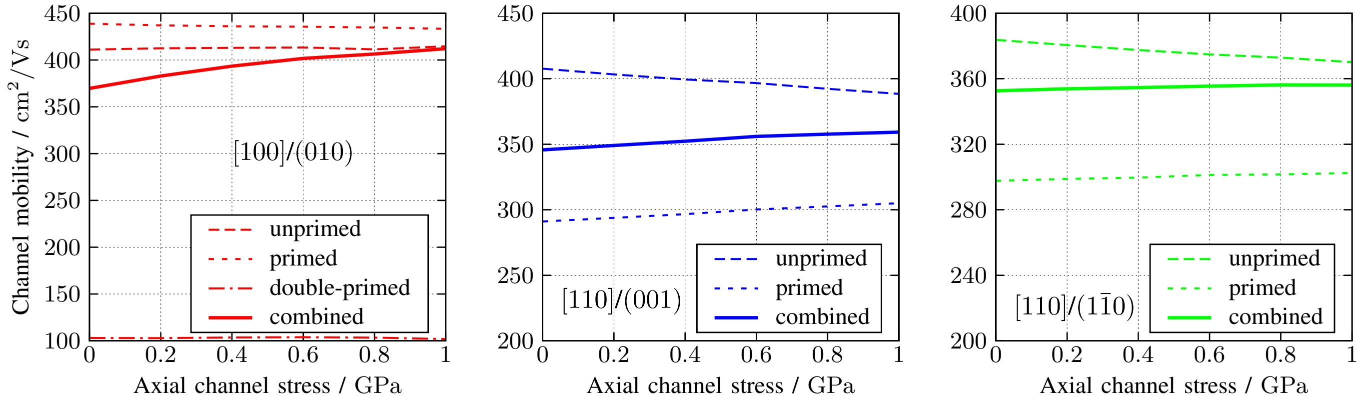

Fig. 7. One way to increase mobility is valley re-population which can be achieved by confinement or strain. Valleys experience different energy shifts from strain depending on their orientation, which alters their population. Enhancement through re-population is possible for $\langle 100 \rangle$ channels only, where tensile stress causes the heavy-transport-mass valley (double-primed) to shift upwards and become less populated. In non-planar channels such as fins the heavy-transport-mass valley is already shifted almost out of reach due to confinement and the mobility is close to its maximum possible value. Thus, mobility enhancement by re-population is diminished in fins compared to planar MOS and UTB channels.

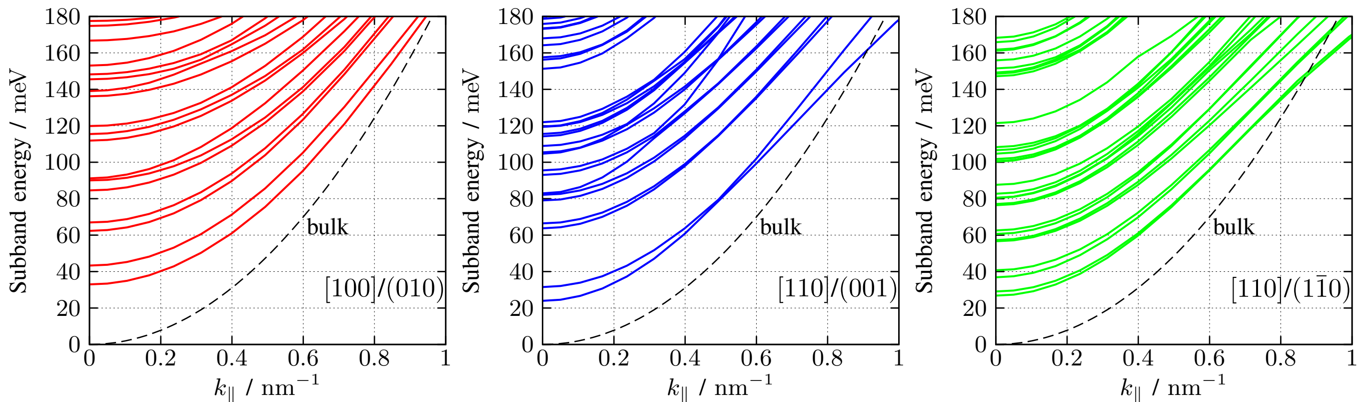

Fig. 8. Another way to affect channel mobility is through subband engineering. Shown are the subband structures as computed using a $\mathbf{k}\cdot\mathbf{p}$ band structure description for different orientations of the 8 nm top width fin. Geometrical and electrostatic confinement both affect the subband structures as do orientation and strain. In the [100]/(010) channel electrons appear heavier than in bulk, whereas in [110]/(001), and [110]/(1$\bar{1}$0) channels effective mass is about the same as in bulk but with increased non-parabolicity.

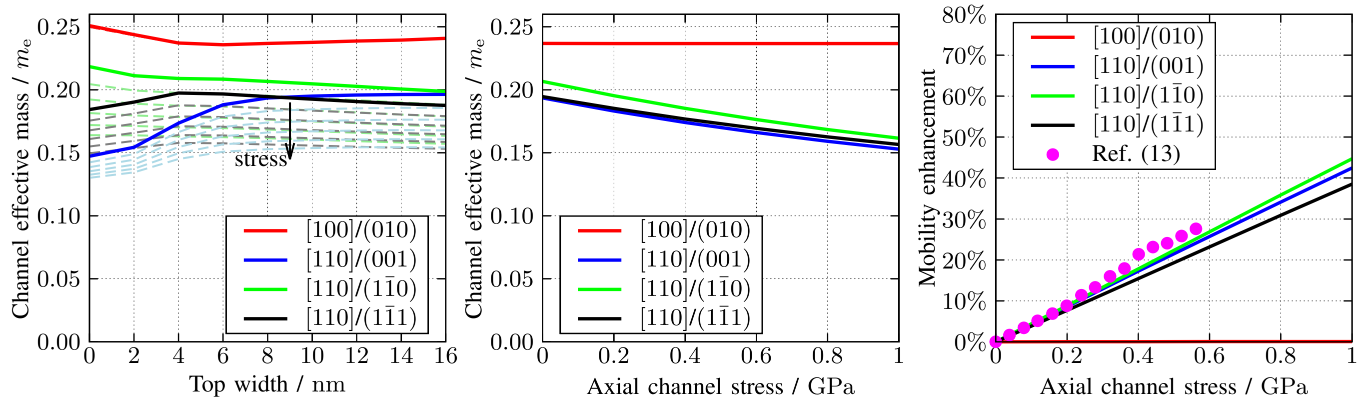

Fig. 9. The key figure is the transport effective mass; a lighter effective mass directly results in higher mobility due to a $\mu \propto m_{\mathrm{eff}}^{-3/2}$ relation in one-dimensional electron gases (15). The increased transport mass in the [100]/(010) channel results in a mobility reduction of $\approx 25\%$ which cannot be reversed using strain. Channels in $\langle 110 \rangle$ direction do not have this penalty; in fact, their transport mass can be reduced below the bulk value by tensile stress along the channel. The resulting mobility enhancement can be as big as $\approx 30\%$ for 600 MPa which is in excellent agreement with experimental observations from (13).